Available online at www.sciencedirect.com
ScienceDirect
Journal of Power Sources 178 (2008) 53–58
JOURNAL OF POWER SOURCES
www.elsevier.com/locate/jpowsour

Short communication

Structural studies of enzyme-based microfluidic biofuel cells

Makoto Togo, Akimasa Takamura, Tatsuya Asai, Hirokazu Kaji, Matsuhiko Nishizawa *

Department of Bioengineering and Robotics, Graduate School of Engineering, Tohoku University, Aoba 6-6-01, Aramaki, Aoba-ku, Sendai, Miyagi 980-8579, Japan

Received 16 November 2007; received in revised form 11 December 2007; accepted 12 December 2007

Abstract

An enzyme-based glucose/O_2 biofuel cell was constructed within a microfluidic channel to study the influence of electrode configuration and fluidic channel height on cell performance. The cell was composed of a bilirubin oxidase (BOD)-adsorbed O_2 cathode and a glucose anode prepared by co-immobilization of glucose dehydrogenase (GDH), diaphorase (Dp) and VK_3-pendant poly-L-lysine. The consumption of O_2 at the upstream cathode protected the downstream anode from interfering O_2 molecules, and consequently improved the cell performance (maximum cell current) ca. 10% for the present cell. The cell performance was also affected by the channel height. The output current and power of a 0.1 mm-height cell was significantly less than those of a 1 mm-height cell because of the depletion of O_2, as determined by the shape of the *E–I* curve at the cathode. On the other hand, the volume density of current and power was several times higher for the narrower cell.

Keywords: Biofuel cell; Vitamin K_3; Diaphorase; Glucose dehydrogenase; Microfluidics

1. Introduction

Various kinds of miniature devices for ubiquitous power supplies have been developed in recent years [1–5]. The enzymatic biofuel cell is one option for such a device because it works under mild conditions: room temperature, neutral pH and atmospheric pressure [6–21] that increase freedom of construction including miniaturization. The enzymatic biofuel cells are composed of a couple; an anode and cathode, modified with an enzyme catalyst and usually an electron transfer mediator, and they generate electric power from an aerobic solution containing biofuel such as glucose. The dissolved molecular O_2 is the substrate of the cathodic enzyme reaction and also acts as the interfering substance for anode reactions. It is experimentally known that the dissolved O_2 can intercept electrons from the anode (enzymes and/or mediators) and consequently lower the externally delivered power. For example, Heller's group has reported that the power density of their biofuel cell in O_2-saturated solution was 30% lower than that in air because of the undesirable electron transfer from glucose oxidase (GOD) to the dissolved O_2 [22–25]. Also, we have studied a glucose anode prepared by co-immobilization of enzymes and vitamin K_3 (VK_3) as an electron mediator [6,9], and reported lower performance in the aerobic solution [6] probably caused by leakage of electrons from enzymes and VK_3 to O_2 molecules. In addition to these energy losses due to reversible reaction with O_2, irreversible oxidative degradation of mediators and enzymes could become serious during longer periods of operation [26]. The simple answer to address these unfavorable reactions of O_2 at the anode is to compartmentize the deoxygenized anode room and oxygenized cathode room by a separator [17] or laminar flow [7]. Such complicated systems, however, may not be suitable to miniature power sources. In contrast, we have another choice to decrease the O_2 flux to the enzymatic anode and that is by electrode-arrangement in the single flow channel. The upstream cathode may deplete O_2 from the vicinity of the downstream anode within a microfluidic channel.

In the work reported in this paper, we constructed an enzyme-based microfluidic biofuel cell composed of a bilirubin oxidase (BOD)-adsorbed O_2 cathode and a glucose anode prepared by co-immobilization of glucose dehydrogenase (GDH), diaphorase (Dp) and VK_3-pendant poly-L-lysine. We studied the effects of pre-electrolysis of O_2 at the upstream cathode on the performance of the downstream anode both experimentally and

* Corresponding author. Tel.: +81 22 217 7003; fax: +81 22 217 3586.
E-mail address: nishizawa@biomems.mech.tohoku.ac.jp (M. Nishizawa).

0378-7753/$ – see front matter © 2007 Elsevier B.V. All rights reserved.
doi:10.1016/j.jpowsour.2007.12.052

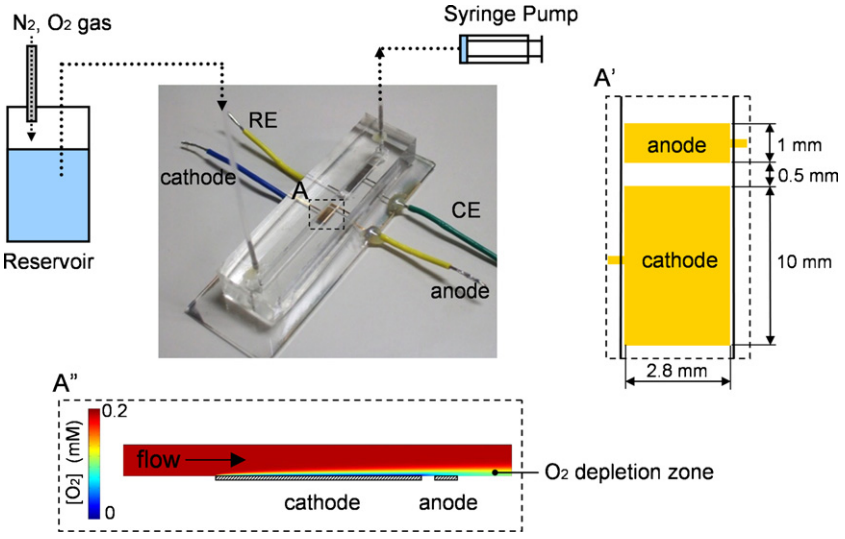

Fig. 1. Schematic illustration and photograph of microfluidic biofuel cell with (A′) the close up top view of the electrodes and (A″) the cross-sectional view of a COMSOL simulation of an O_2 depletion layer forming along the channel.

theoretically under regulated conditions: flow velocity, electrode length, electrode gap and channel height. Based on the results obtained, the optimum design of a fluidic cell will be discussed from the aspects of power and power density.

2. Experimental

2.1. Reagents

The synthesis of the redox polymer VK_3-modified poly-L-lysine (PLL-VK_3) has been described previously [6]. The diaphorase (Dp) from *Bacillus stearothermophilus* (EC 1.6.99, 1090 U mg^{-1}) was purchased from Unitika. NAD^+-dependent glucose dehydrogenase (GDH; EC 1.1.1.47, 250 U mg^{-1}) was donated by TOYOBO. Bilirubin oxidase (BOD) from *Myrothecium sp.* (EC 1.3.3.5, 2.45 U mg^{-1}) was purchased from Amano Enzyme Inc. Ketjenblack (KB; EC-600JD) was supplied by Ketjen Black International, Inc. NAD^+ was used as received from Oriental Yeast Co.

2.2. Electrodes preparation

A PLL-VK_3/Dp/GDH-coated KB electrode was prepared as previously reported [6]. A brief description of the preparation follows. Unless otherwise indicated, the enzyme solutions for electrode modification were prepared using 50 mM phosphate buffered solution (pH 7.0). An 8 μL PLL-VK_3 solution (4.83 mM VK_3) was mixed with a 2 μL Dp solution (14 μg $μL^{-1}$) and 1 μL of KB dispersed water (ca. 13 mg mL^{-1}). A 5.3 μL portion of the resulting solution was put onto a gold film electrode (surface area, 0.028 cm^2) on a glass substrate, and was left to dry in air. To create the enzymatic bilayer, the surface of a PLL-VK_3/Dp-coated KB electrode was coated with 1.6 μL of a solution composed of equal volumes of a 16 μg $μL^{-1}$ GDH solution and a 16 mg mL^{-1} PLL solution.

A BOD-adsorbed KB electrode was prepared as described below. A mixture of 3:1 weight ratio of KB and poly(tetrafluoroethylene) (MW 5000–20,000, Wako) was dispersed in isopropanol (2 mg mL^{-1}), and applied to a gold electrode (0.11 mL cm^{-2}) followed by overnight drying in a 70 °C oven. And then, BOD was adsorbed to the KB electrode by dipping in the 5 mg mL^{-1} BOD solution for 10 min and washed with phosphate buffer solution for 10 min. The measurement was carried out before the BOD-modified electrode dried completely because the BOD loses its activity in the dry state [27,28].

2.3. Microfluidic biofuel cell and electrochemical measurements

We constructed microfluidic fuel cells of the type shown in Fig. 1. Film electrodes were patterned on the surfaces of glass slides by photolithography and spattering, which is a lift-off process. Both anode's (2.8 mm width, 1 mm long) and cathode's (2.8 mm width, 10 mm long) Au current collectors were modified by KB and enzymes. The gap between anode and cathode was 0.5 mm. The Ag|AgCl electrode was fabricated by coating a Pt film with Ag|AgCl ink (BAS Inc.) that was then cured at 80 °C for 2 h. A negative of the channel shape was prepared by thick photoresist (SU-8 2050, Microchem) by photolithography and transcribed to polydimethylsiloxane (PDMS; SYLPOT 184 W/C, Dow Corning Toray) slabs, so as to producing channels of 3 mm width and 0.1 mm or 1 mm height.

All electrochemical measurements were performed in 50 mM phosphate buffer solution (pH 7.0) containing 0.1 M NaCl at room temperature. The electrochemical properties of the electrodes were characterized using a bipotentiostat (Electrochemical Analyzer, Model 600S, BAS) with three electrode system containing an enzyme-modified electrode as the working electrode, an Ag|AgCl (0.1 M NaCl) reference electrode and a platinum counter electrode. The fuel cell performance was evaluated by measuring the cell voltage while varying the external

resistance between 5 and 200 kΩ. When we evaluated the electrode performance in the various O_2 concentration solutions, we bubbled the reservoir solution with N_2 or O_2. A micro syringe pump (Kd Scientific, Model 210) was used to make a steady flow in the microfluidic channel. The Reynolds number of the flow was small enough to maintain laminar flow.

2.4. Numerical simulations

To asses the shape of the depletion zone of the O_2 in the fluidic channel, we simulated a microfluidic biofuel cell using finite element method software COMSOL multiphysics 3.1 (COMSOL AB) (Fig. 1A″). The simulation was carried out by coupling the Navier–Stokes equation, continuity equation and the mass balance equation, assuming the flow velocity at the surface of the wall is zero (non-slip flow) and O_2 concentration at the surface of the cathode is zero. The diffusion coefficient of O_2 was set to 2×10^{-9} m^2 s^{-1} [27], the bulk concentration of O_2 to 0.2 mol m^{-3}, the fluid density to 1×10^3 kg m^{-3}, fluid viscosity to 1×10^{-3} kg m^{-1} s^{-1} and the average flow velocity to 1.7×10^{-3} m s^{-1}. Channel height and cathode length were set to 1 mm and to10 mm, respectively.

3. Result and discussion

3.1. Linear sweep voltammetry of anode and cathode in a microfluidic channel

Fig. 2a shows linear sweep voltammograms (LSVs) of glucose anode (2.8 mm^2) in 0.3 mL min^{-1} (10 cm min^{-1}) flow of N_2-bubbled phosphate buffer solution containing 10 mM glucose and 1.0 mM NAD$^+$ (···), with a sigmoidal shape reaching 27 μA (ca. 1 mA cm^{-2}). The glucose oxidation current depends on the flow rate as previously reported [6]. The higher flow rate leads to higher current. The glucose oxidation currents obtained in air-saturated solution (—) and O_2-saturated solution (- - -) were somewhat smaller than that in N_2-bubbled solution, probably because the dissolved O_2 competes with electron relay at the PLL-VK$_3$/Dp/GDH/KB electrode. In addition to this short-term adverse effect of dissolved O_2 to anode, the irreversible oxidative degradation would occur during longer operation.

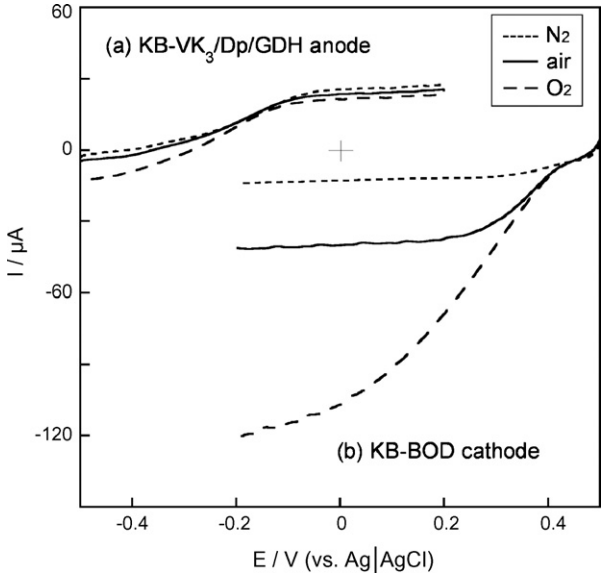

Fig. 2. LSVs of (a) anode and (b) cathode in N_2-bubbled (···), air-saturated (—), and O_2-bubbled (- - -) 50 mM phosphate buffer (pH 7) containing 0.1 M NaCl, 1 mM NAD$^+$ and 10 mM glucose at room temperature, with a flow rate of 0.3 mL min^{-1}. Scan rate: 2 mV s^{-1}. Channel height: 1 mm.

The LSVs of BOD-adsorbed KB electrode (10 mm long, 28 mm^2) are shown in Fig. 2b. In N_2-bubbled solution (···), only a small current was observed, but in air-saturated (—) and O_2-bubbled solution (- - -), the O_2 reduction catalytic current clearly appeared at a potential more negative than 0.45 V. The starting potential of O_2 reduction current was about 0.2 V more positive than for the case with Pt electrode as the cathode [6]. This superior performance of a BOD-modified electrode has been already reported by Tsujimura and Kano [8,27–30]. This was due to the direct electron transfer of BOD. The catalytic current reached 41 μA in air saturated solution and 120 μA in O_2-bubbled solution. The shape of LSV was not influenced by the additional presence of NAD$^+$ and glucose owing to the satisfying reaction selectivity of KB/BOD electrode to O_2 reduction. We have set the flow rate at 10 cm min^{-1}, where the diffusion layer of O_2 grows up to a few hundred μm but does not cover the 1 mm channel height, as theoretically discussed later.

As described above, we measured the polarization curve of the glucose electrode and O_2 electrode individually under operating conditions of the fuel cell by using the microfluidic biofuel cell system that internally contains a reference electrode and a counter electrode. In order to balance the current at anode and cathode, we set the area of the cathode (28 mm^2) ten times larger that the anode (2.8 mm^2). The combination of these electrodes is expected to show OCV of ca. 0.8 V and maximum current of ca. 25 μA (as limited by anode) in the air-saturated glucose solution. This expected cell performance could be obtained only if the anode is protected from O_2 without decreasing O_2 flux to the cathode.

3.2. O_2 reduction at upstream cathode

With the aim of decreasing the O_2 flux to the anode as simulated in Fig. 1A″, we experimentally studied the effect of pre-reduction of O_2 at a cathode set upstream of the fluidic channel. Fig. 3a shows the currents at the downstream glucose anode versus the O_2 reduction current at the upstream cathode. The glucose oxidation current (at 0 V vs. Ag|AgCl) was successfully increased by the pre-reduction of O_2 by up to 23 μA, nearly equal to that observed in the N_2-bubbled solution (- - -), suggesting that the degree of decrease in O_2 flux in the vicinity of the anode was sufficient to prevent the adverse reaction of O_2. The pre-reduction should become more significant at lower glucose concentration or higher O_2 concentration due to the relatively larger flux of competitive O_2. The O_2 flux downstream was estimated by experiments using the KB/BOD electrode for both upstream and even downstream (Fig. 3b). The O_2 reduction current (at −0.4 V vs. Ag|AgCl) at the downstream KB/BOD electrode ($I_{O_2 \text{ at downstream}}$) decreased linearly with increasing

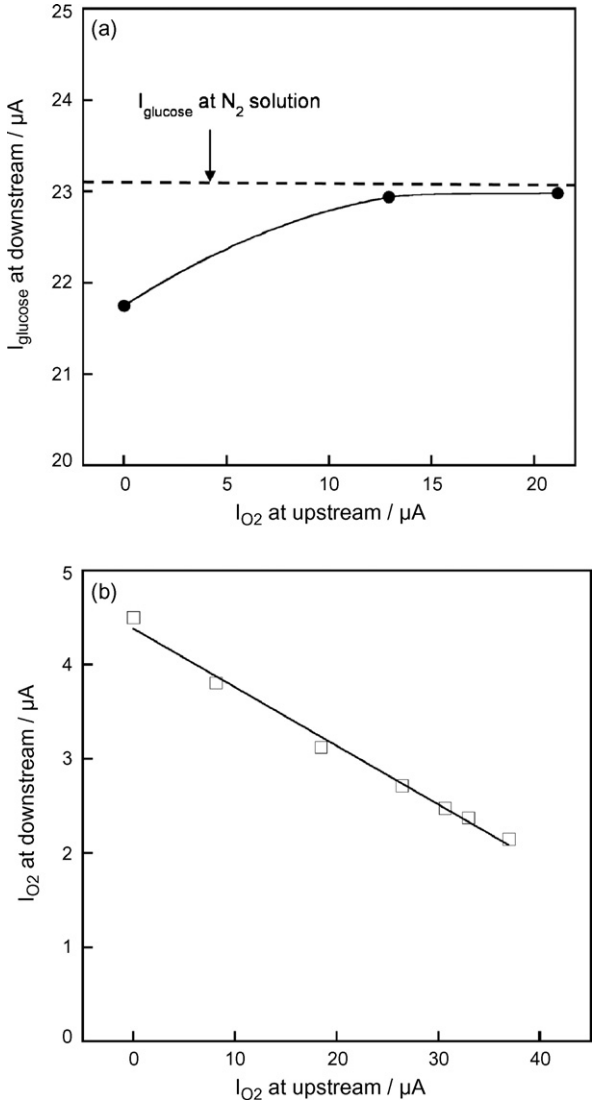

Fig. 3. (a) Glucose oxidation current of downstream glucose anode ($I_{glucose}$ at downstream) vs. O_2 reduction current of upstream BOD cathode (I_{O_2} at upstream), and (b) O_2 reduction current of downstream BOD electrode (I_{O_2} at downstream) vs. O_2 reduction current of upstream BOD electrode (I_{O_2} at upstream), measured in the phosphate buffer (pH 7) containing 0.1 M NaCl, 10 mM glucose and 1 mM NAD^+ at room temperature, with a flow rate of 0.3 mL min^{-1}. Channel height: 1 mm.

pre-reduction current ($I_{O_2 \text{ at upstream}}$). This linear relationship can be expressed as the equation,

$$i_{\text{downstream}} = i^0_{\text{downstream}} - Ni_{\text{upstream}} \quad (1)$$

where $i^0_{\text{downstream}}$ is the current at the downstream electrode when $i_{\text{upstream}} = 0$, and N is the efficiency of O_2 elimination estimated as 0.065 from the decay of the plot. The experimental N value (0.065) is unfortunately inferior to the theoretical one (Nth = 0.13) calculated by the equation for the channel flow electrode system [31], probably because of unknown factors affecting N: e.g., the thickness (several tens of μm) and roughness of the KB electrodes. The Nth is the function of only electrode configuration [31], and suggests that a higher Nth would be obtained by a narrower electrode gap and smaller

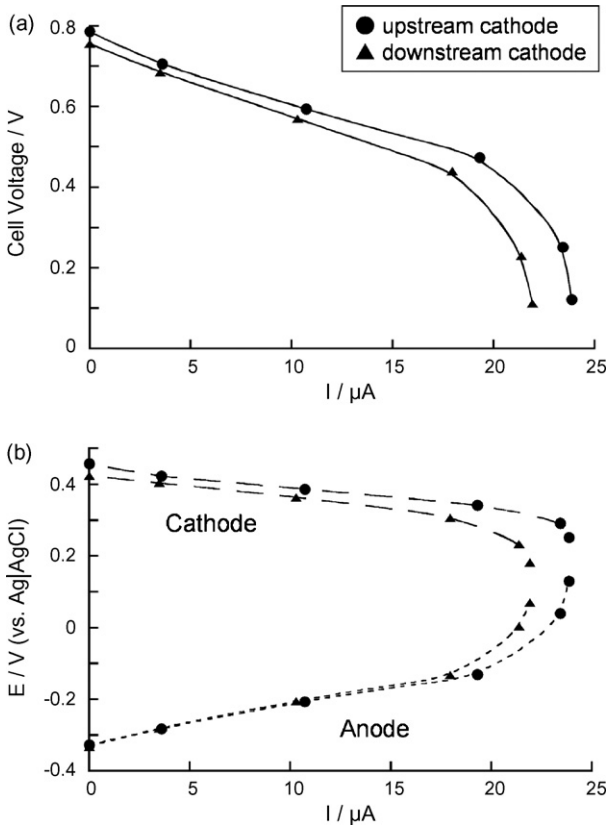

Fig. 4. (a) *V–I* curve of microfluidic biofuel cell (—), and (b) *E–I* curves of anode (···) and cathode (- - -) operating under air-saturated phosphate buffer (pH 7) containing 0.1 M NaCl, 10 mM glucose and 1 mM NAD^+ at room temperature, with a flow rate of 0.3 mL min^{-1}. The cells were operated with upstream cathode (●) or downstream cathode (■). Channel height: 1 mm.

upstream cathode, while the small cathode has the disadvantage for generating larger power.

3.3. Microfluidic biofuel cell performance

By connecting enzymatic anode and cathode through external resistance, biofuel cell performance was evaluated for 0.3 mL min^{-1}. Fig. 4a shows the cell performance (*V–I* curve) in an air-saturated solution with an open circuit voltage (V_{oc}) of around 0.8 V and maximum current (I_{max}) of over 20 μA. This is in agreement with the prediction from performance of each anode and cathode (Fig. 2). The *V–I* curve obtained with the upstream-cathode cell (●) was bigger than that with the downstream-cathode cell (▲), especially in the higher current region. The I_{max} increased 10% by placing the cathode upstream, mainly reflecting the improved anode as judged from the analogy between the shape of the *V–I* curve of the cell (—) and the *E–I* curve of the anode (···). The E-I curve of the cathode (- - -) was also somewhat changed, indicating the consumption of O_2 at the upstream anode by the adverse reaction with enzymes and mediators. Another separate experiment with an O_2-bubbled solution brought smaller I_{max} (ca. 20 μA) due to the larger O_2 flux to the upstream anode, which was improved 15% by pre-reduction of O_2 at the upstream cathode. These results have proven that the cell design with upstream cathode is effective in protect-

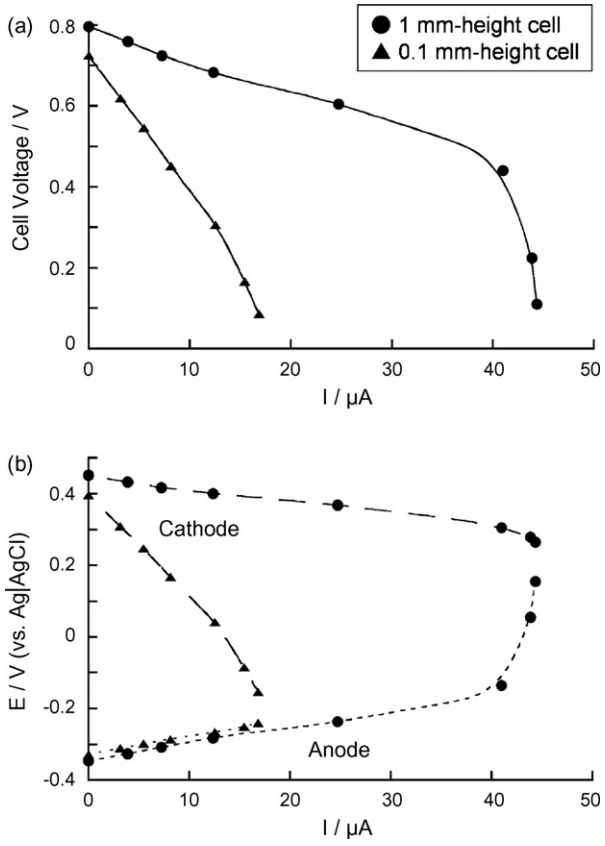

Fig. 5. (a) *V–I* curves of sandwich type microfluidic biofuel cell (—), and (b) *E–I* curves of anode (· · ·) and cathode (- - -) operating under air-saturated phosphate buffer (pH 7) containing 0.1 M NaCl, 10 mM glucose and 1 mM NAD^+ at room temperature, with a mean flow rate of 10 cm min^{-1}. Channel height: 1 mm (●) and 0.1 mm (■).

ing the anode from the oxidative environment and consequently improving cell performance.

We also studied the performance of microfluidic biofuel cells having electrodes on both bottom and upper walls of the channel (Fig. 5). These were constructed by sandwiching a silicone rubber spacer of 0.1 mm or 1 mm thickness between two electrode-patterned glass slides. Both glass slides have a set of upstream cathode and downstream anode. The I_{max} of the 1 mm-height cell (44 μA) was almost twice that for the case of a single set of electrodes as shown in Fig. 4. This result directly corresponds to the increased electrode area. In contrast, the I_{max} of 0.1 mm-height cell (▲) composed of two sets of electrodes became rather small mainly because of depletion of O_2 in the narrower flow channel, as presumed from the degraded cathodic *I–E* curve. Theoretically, at the maximum diffusional flux ($c = 0$ at the electrode surface), the thickness of the diffusion boundary layer δ (cm) formed on the electrode within a tube-shaped channel is expressed as [32],

$$\delta = \frac{1}{0.67}\left(\frac{DRx}{v_0}\right)^{1/3} \quad (2)$$

where D is the diffusion coefficient ($cm^2\ s^{-1}$), R the radius of the tube, x the distance measured downstream from the leading edge of the electrode (cm) and v_0 is the maximum velocity at the axis of the tube ($r = 0$) (cm s^{-1}). From Eq. (2), the thickness of the O_2 depletion layer under the flow condition of 10 cm min^{-1} (0.3 mL min^{-1}) is calculated to be about several hundred μm at a position 1 mm-downstream from the leading edge of the cathode, which can fully cover the 0.1 mm-height fluidic channel and lower cell performance. On the other hand, from the viewpoint of the "volume density", the 0.1 mm-height narrower cell is superior to the 1 mm-height cell; the volume density of I_{max} and P_{max} of the 0.1 mm-height cell was 3.8 times and 2 times, respectively, as large as those of the 1 mm-height cell. The optimum efficient operation with the highest density of output would be at the flow condition forming depletion layer comparable to the channel height.

4. Conclusion

We constructed an enzyme-based microfluidic biofuel cell to study the effects of pre-electrolysis of O_2 at the upstream cathode on the performance of the downstream anode under regulated fluidic conditions. The upstream cathode successfully reduced the O_2 flux to the anode, and consequently improved the glucose oxidation performance. The maximum cell current with the upstream-cathode cell was about 10% higher than that with the downstream-cathode cell. It was experimentally demonstrated that, we need to take into account the depletion of fuel and oxidant within the channel that depends on the channel height and flow rate in addition to the electrode configuration. One of the optimum operating conditions would be when the flow forming depletion layer is comparable to the channel height. The active O_2 supply from external air through the channel wall should be effective in improving the cell performance. In such an O_2-concentrated condition, the cell construction with upstream cathode would become more significant to maintain anode's performance.

Acknowledgements

This work was partly supported by Health and Labor Sciences Research Grant from the Ministry of Health, Labor and Welfare of Japan.

References

[1] K.B. Lee, J. Micromech. Microeng. 15 (2005) S210–S214.
[2] K.B. Lee, L.W. Lin, J. Microelectromech. Syst. 12 (2003) 840–847.
[3] R.S. Jayashree, L. Gancs, E.R. Choban, A. Primak, D. Natarajan, L.J. Markoski, P.J.A. Kenis, J. Am. Chem. Soc. 127 (2005) 16758–16759.
[4] E.R. Choban, L.J. Markoski, A. Wieckowski, P.J.A. Kenis, J. Power Sources 128 (2004) 54–60.
[5] R. Ferrigno, A.D. Stroock, T.D. Clark, M. Mayer, G.M. Whitesides, J. Am. Chem. Soc. 124 (2002) 12930–12931.
[6] M. Togo, A. Takamura, T. Asai, H. Kaji, M. Nishizawa, Electrochim. Acta 52 (2007) 4669–4674.
[7] K.G. Lim, G.T.R. Palmore, Biosens. Bioelectron. 22 (2007) 941–947.
[8] Y. Kamitaka, S. Tsujimura, N. Setoyama, T. Kajino, K. Kano, PCCP Phys. Chem. Chem. Phys. 9 (2007) 1793–1801.
[9] F. Sato, M. Togo, M.K. Islam, T. Matsue, J. Kosuge, N. Fukasaku, S. Kurosawa, M. Nishizawa, Electrochem. Commun. 7 (2005) 643–647.
[10] C.M. Moore, S.D. Minteer, R.S. Martin, Lab Chip 5 (2005) 218–225.

[11] A. Heller, AiChE J. 51 (2005) 1054–1066.
[12] A. Heller, PCCP Phys. Chem. Chem. Phys. 6 (2004) 209–216.
[13] S.C. Barton, J. Gallaway, P. Atanassov, Chem. Rev. 104 (2004) 4867–4886.
[14] N. Mano, F. Mao, W. Shin, T. Chen, A. Heller, Chem. Commun. (2003) 518–519.
[15] S. Tsujimura, K. Kano, T. Ikeda, Electrochemistry 70 (2002) 940–942.
[16] N. Mano, F. Mao, A. Heller, J. Am. Chem. Soc. 124 (2002) 12962–12963.
[17] S. Tsujimura, M. Fujita, H. Tatsumi, K. Kano, T. Ikeda, PCCP Phys. Chem. Chem. Phys. 3 (2001) 1331–1335.
[18] E. Katz, A.F. Buckmann, I. Willner, J. Am. Chem. Soc. 123 (2001) 10752–10753.
[19] T. Chen, S.C. Barton, G. Binyamin, Z.Q. Gao, Y.C. Zhang, H.H. Kim, A. Heller, J. Am. Chem. Soc. 123 (2001) 8630–8631.
[20] G.T.R. Palmore, H. Bertschy, S.H. Bergens, G.M. Whitesides, J. Electroanal. Chem. 443 (1998) 155–161.
[21] T. Tamaki, T. Ito, T. Yamaguchi, J. Phys. Chem. B 111 (2007) 10312–10319.
[22] N. Mano, F. Mao, A. Heller, J. Electroanal. Chem. 574 (2005) 347–357.
[23] N. Mano, A. Heller, Anal. Chem. 77 (2005) 729–732.
[24] N. Mano, F. Mao, A. Heller, J. Am. Chem. Soc. 125 (2003) 6588–6594.
[25] H.H. Kim, N. Mano, X.C. Zhang, A. Heller, J. Electrochem. Soc. 150 (2003) A209–A213.
[26] H. Tatsumi, H. Nakase, K. Kano, T. Ikeda, J. Electroanal. Chem. 443 (1998) 236–242.
[27] S. Tsujimura, K. Kano, T. Ikeda, J. Electroanal. Chem. 576 (2005) 113–120.
[28] S. Tsujimura, T. Nakagawa, K. Kano, T. Ikeda, Electrochemistry 72 (2004) 437–439.
[29] Y. Kamitaka, S. Tsujimura, K. Kataoka, T. Sakurai, T. Ikeda, K. Kano, J. Electroanal. Chem. 601 (2007) 119–124.
[30] M. Tominaga, M. Otani, M. Kishikawa, I. Taniguchi, Chem. Lett. 35 (2006) 1174–1175.
[31] T. Tsuru, Mater. Sci. Eng. A: Struct. Mater. Prop. Microstruct. Process. 146 (1991) 1–14.
[32] V.G. Levich, Physicochemical Hydrodynamics, Prentice-Hall, Inc., Englewood Cliffs, NJ, 1962.